



Fatigue analysis of steel catenary riser at the touch-down point based on linear hysteretic riser-soil interaction model



Kunpeng Wang^a, Hongxiang Xue^{a,*}, Wenyong Tang^a, Jinting Guo^b

^a State Key Laboratory of Ocean Engineering, Shanghai Jiao Tong University, Shanghai 200240, China

^b Naval Architecture and Marine Engineering, University of Michigan, Ann Arbor, MI 48109, USA

ARTICLE INFO

Article history:

Received 21 September 2011

Accepted 6 April 2013

Available online 18 May 2013

Keywords:

SCR touch-down point

Linear hysteretic seabed model

Fatigue damage

Seabed strength

Seabed suction

Trench effect

ABSTRACT

The fatigue life of a steel catenary riser (SCR) at the touch-down point (TDP) is substantially affected by its interaction with the seabed. In order to broaden the understanding of seabed effects on TDP's fatigue performance and provide more accurate fatigue life prediction in the SCR's design, the effects of the seabed characteristics on fatigue damage of the SCR at the TDP have been studied in this paper. In this study, a new element at touch-down zone (TDZ) is created to simulate the riser-soil interaction based on the proposed linear hysteretic riser-soil interaction model. A conventional twin-pontoon semi-submersible with a particular riser geometry in the South China Sea, is adopted to evaluate how the fatigue damage was affected by the seabed characteristics. The results based on this study indicate that: ① Larger mudline shear strength and shear strength gradient corresponding to stiffer seabed lead to shorter fatigue life. ② The seabed suction effect could not be neglected in the SCR's design, since its effect on the TDP's fatigue damage is obvious and the greater suction force causes more fatigue damage. ③ The deeper the trench, the less TDP's fatigue damage will be. Therefore the development of trench is in favor of longer fatigue life of the riser.

© 2013 Elsevier Ltd. All rights reserved.

1. Introduction

Steel catenary risers (SCRs) are an enabling technology for the deepwater oil and gas production and they are compatible with many host types (i.e. Semi-submersible, Spar, TLP and FPSO). Nowadays there are more than 100 SCRs installed in West of Africa, Gulf of Mexico, offshore Brazil and so on. As a matter of fact, the deeper water and the bigger diameter of the riser, the more difficult for SCR's design will be due to the nonlinearity of the riser and the applied loads.

Fatigue life is one of the important parameters for SCR's design. The previous studies show that the TDP, where the SCR starts to contact the seabed, is one of the critical locations of SCR prone to fatigue failure (Fu et al., 2010). In order to accurately estimate the fatigue life of a SCR at its TDP, a reasonable seabed model is required. However, traditional studies generally use either rigid connection or elastic spring to approximate the behavior of the seabed soil due to the complication of riser-soil interaction and unknown trench development mechanism, which could lead to a non-realistic fatigue life prediction.

* Correspondence to: No. 800, Dongchuan Road, School of Naval Architecture, Ocean & Civil Engineering, Shanghai Jiao Tong University, Shanghai, 200240, China. Tel.: +86 021 34206579; fax: +86 021 34206642.

E-mail address: hongxiangxue@sjtu.edu.cn (H. Xue).

When riser is lifted up from trench, TDZ will experience soil suction that involves three stages: suction mobilization, suction plateau and suction release (Bridge and Willis, 2002; Bridge and Laver, 2004). The process of riser-seabed interaction for each period can be divided into four subsections including re-contact, elastic rebound, partial soil-pipe separation and full separation, and each subsection can be presented by empirical formulas (Aubeny et al., 2006). Induced by the oscillating floating structure, the SCR near its TDP periodically touch the seabed, which results in deeper and deeper trench. The study of Nakhaee and Zhang (2010) indicates that deeper trench gives lower bending moment at touch-down zone. In addition, Vortex Induced Vibration analysis of SCRs considering the riser-seafloor interaction was conducted in Larsen and Passano (2006), where the seabed was simulated as the springs. Although researchers have made great progress in soil-seabed interaction studies, due to the difficulty in numerical simulation of seabed characteristic, there is limited study focusing on the effects of the seabed characteristics on the TDP's fatigue damage.

Frequency domain method is often used to calculate fatigue life of a riser for relatively low computational cost. Based on linear wave theory, Fan et al. (2008) applied spectral method to study the fatigue life of top tension risers (TTRs). Power et al. (2008) compared the fatigue life derived from the spectral method and the time domain method. Although the results matched well, there is no detailed information about how to model the riser-soil

interaction and the coupled effect between SCR and platform. Generally, the seabed and the coupled effect between SCR and the platform should be modeled accurately to provide a good fatigue life prediction of SCRs at the TDP. Therefore, the coupled nonlinear time domain method is preferred and used for this study.

By combining the nonlinear hysteretic model 2H Offshore Engineering Ltd (2002) and the seabed plastic degradation model (Aubeny and Biscontin, 2008), a linear hysteretic riser-soil interaction model is proposed in this study. Compared with the riser-soil interaction model used in Orcaflex software (Randolph and Quiggin, 2009), several different considerations are applied in this model. First, it linearizes the subsection of the nonlinear hysteretic model. Second, it applies the beam-spring equilibrium to form an approximate initial trench. Since the trench development is very slow and the simulation time is limited in the detail analysis for SCRs, it is acceptable to simulate a trench with a certain depth in the global analysis. In order to consider the coupled effect between the SCR and the platform, a hydrodynamic program, DeepC (DNV, 2005a), is used to obtain the upper end motion of the SCR, which is then applied as the top boundary condition for the detail nonlinear analysis in ABAQUS/Standard (ABAQUS, 2005). The complex soil-riser interaction is then simulated by a user-defined TDZ element based on the linear hysteretic seabed model.

2. Hull/mooring/riser coupled system

The selected semi-submersible hull has two-pontoons connected with four columns. Its principal dimensions are presented in Table 1. The platform system is equipped with a 12-point spread mooring system with the form of chain-wire-chain, and one SCR.

The SCR in the study works in a water depth of 1219.2 m. Detail particulars of the SCR is presented in Table 2. D_{out} and D_{in} are nominal outer and inner diameters, C_m and C_D are inertia and drag coefficients respectively.

3. Fatigue analysis

3.1. Environmental loads

Deep water SCRs are subjected to complicated environmental loads, including Morison load, VIV, installation load, seabed restriction, and coupled motion with hull. VIV and installation load are not considered in this paper.

The semi-submersible platform system serves in the South China Sea where the wave scatter diagram is divided into six blocks, from which six short term sea states are selected to simulate the wave environment. This paper assumes that the waves from different directions have the equal occurrence probability, and the current speed does not change with the sea state. the selected short sea states and current information are shown in Tables 3 and 4 respectively.

Table 1
Principles of the Semi-submersible.

Hull structure length overall	114	m
Hull structure width overall	78	m
Pontoon length	114	m
Pontoon width	9.2	m
Column width	17.4	m
Column length	38	m
Operational/Survival draft	19	m
Displacement	51700	mT
Vertical buoyancy center	−12.4	m
Vertical CoG	9.2	m

Table 2
Principles of SCR.

Length	2050	m
Top hang off angle	14	deg
Fluid density	881	kg/m ³
Wet weight	118.9	kg/m
Dry weight	177.6	kg/m
D_{out}	0.27	m
D_{in}	0.21	m
C_m	2	
C_D	0.7	

Table 3
Short term sea state for fatigue analysis.

Sea state no.	Significant wave height H_s (m)	Wave peak period T_p (s)	Wind velocity V_w (m/s)	Surface current velocity V_c (m/s)	Occurrence probability
LC1	1.25	5.3	8	0.9	0.534
LC2	1.75	5.3	9	0.9	0.18
LC3	2.25	5.3	10	0.9	0.117
LC4	2.75	5.3	11	0.9	0.0774
LC5	3.75	7.5	12	0.9	0.0516
LC6	4.25	7.5	13	0.9	0.0401

Table 4
Current data.

Distance from seabed (m)	x-velocity (m/s)	y-velocity (m/s)
0.00	0.10	0.00
1128.20	0.56	0.00
1159.20	0.75	0.00
1219.20	0.90	0.00

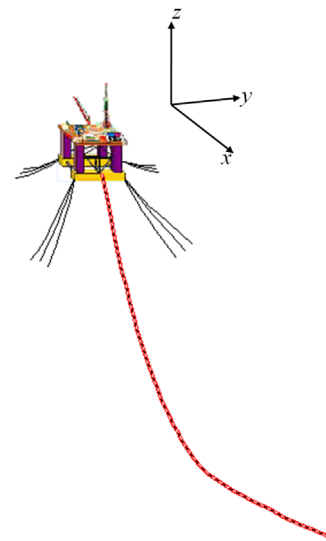


Fig. 1. Full coupled Semi-submersible platform and mooring/SCR.

WADAM(DNV, 2005b), a diffraction/radiation code, is utilized to calculate the frequency-dependent coefficient, such as added mass, radiation damping, first-order wave-excitation forces. The corresponding forces are converted to the time domain using two-term Volterra series expansion. The frequency-dependent radiation damping is included in the form of a convolution integral in Deep C. Fig. 1 shows the global configuration of the platform and mooring/riser system, in which the body fixed coordinate origin is

on the mean water surface at where the line crosses the centroid of hull, and the z -axis is positive upward. After the coupled hydrodynamic analysis, the upper end response of the SCR is obtained to perform a detailed global FE analysis in ABAQUS.

Morison rule is applicable for the SCR, the wave and current loading could be expressed as

$$f = \frac{1}{2} \rho C_D D |U - U_b| (U - U_b) + \rho C_m A (\dot{U} - \dot{U}_b) + \rho A \ddot{U}_b \quad (1)$$

where U and \dot{U} are velocity and acceleration of the fluid respectively, U_b and \dot{U}_b are velocity and acceleration of the riser element respectively.

3.2. Applied fatigue methodology

The S – N approach has been widely used to solve the fatigue problem. To obtain the fatigue life of a SCR at its TDP, it is assumed that the material behavior could be well represented by D curve specified in DNV-RP-C203 (DNV, 2010a). This can be expressed as:

$$N = A[(\Delta S \times SCF (t/t_{ref})^k)]^{-m} \quad (2)$$

where N is the permissible number of cycles for an applied cyclic stress range ΔS in MPa, SCF is the stress concentration factor, which is assumed to be 1.0 in this study, A and m are material constants, t/t_{ref} is the thickness correction factor, the reference thickness t_{ref} equals 25 mm.

According to DNV-RP-F204 (DNV, 2010b), the governing cyclic nominal stress, σ for pipe is a linear combination of the axial (σ_a) and bending stress (σ_M) given by:

$$\sigma = \sigma_a + \sigma_M \quad (3)$$

The σ_a and σ_M are calculated from axial force and bending moment respectively, and then the cyclic stress range can be obtained from the time history response by rainflow method.

To obtain the fatigue damage, the Palmgren–Miner linear damage accumulation hypothesis (Miner's rule) is applied. If the number of selected sea states is NS , and M_i represents the number of different cyclic stress range, ΔS_{ik} repeating n_{ik} cycles in the i th sea state, then the accumulated fatigue damage could be expressed as:

$$D_{acc} = \sum_{i=1}^{NS} \left(\sum_{k=1}^{M_i} n_{ik}/N_{ik} \right) P_i \quad (4)$$

where N_{ik} is the permissible number of cycles for an applied cyclic stress range, ΔS_{ik} in MPa, and P_i is the occurrence probability of the i th sea state. D_{acc} is the fatigue accumulation damage.

4. TDZ element model for the riser-soil interaction simulation

4.1. Introduction of TDZ element model

According to STRIDE JIP (2H Offshore Engineering Ltd, 2002), Bridge and Laver (2004) proposed a conservative large displacement soil stiffness model and a soil stiffness model taking into consideration of the soil suction force, which are presented by the single dot dash line ④ and the dash line ② respectively in Fig. 2. The seabed stiffness of both models is larger than that of the actual seabed, and the mobilization and release of suction are not included. In addition, the accumulation of the plastic deformation after many cycles is also neglected. Actually, the plastic deformation is substantial and should not be neglected (Nakhaee and Zhang, 2010), which could be empirically formulated as follows:

$$(\delta y/D)_{acc} = \beta (\ln N)^\gamma \quad (5)$$

where δy is accumulation plastic deformation after N cycles, D is outer diameter of riser, both γ and β are test parameters.

In this study a linear riser-seabed vertical interaction model, following the dash line cycle (① → ② → ③) shown in Fig. 2, is proposed. In order to simulate the trench development, the degradation model as depicted by eq. (5) is considered. After the SCR touch the seabed several times, the riser-soil interaction model is updated to the loop enclosed by the double dot dash lines. The seabed resistance and suction force during one periodic oscillation are well determined by this model through several parameters, i.e. mudline shear strength S_0 , shear strength gradient S_g , and the maximum suction factor. The definitions of main parameters are presented in Table 5. The characteristics of seabed, current and the dimension of the SCR have significant effects on the trench development and its shape, which determine the model parameters directly. In this study, it is assumed that the risers and soil are separated at the seabed surface and the position factor of the maximum suction is equal to 0.7.

It has been observed that the depth of several trenches in Auger and Allegheny Gulf of Mexico field reach 4–5 times the riser diameters within a few months after the installation (Willis and West, 2001; Thethi and Moros, 2001). Therefore, the trench modeling becomes very important in order to obtain the realistic response near TDZ. The degradation model could simulate the trench development, but the simulation is very time consuming. In order to conduct a design analysis within a reasonable time frame, a certain depth initial trench can be assumed before the global response analysis starts. In this study, $y_{initial,max}$ is used in the equivalent beam-spring model to form an initial trench, and the beam-spring model is governed by the following nonlinear, fourth order ordinary differential equation:

$$EI(d^4y/dx^4) = W - P \quad (6)$$

where E is the young's modulus, I is the sectional moment of inertia, W is the wet weight of the riser per unit length, P is the resistance force per unit riser length obtained from the backbone

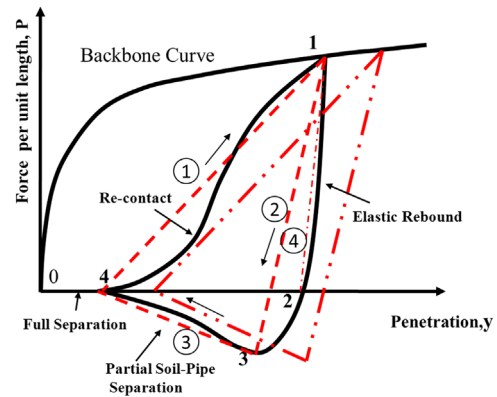


Fig. 2. Typical p – y curve.

Table 5
Parameters of TDZ element modeling.

Particulars	Definition
$y_{initial,max}$	Maximum initial depth of trench for beam-spring model
S_0	Seabed mudline shear strength
S_g	Seabed shear strength gradient
μ_{sep}	Riser-soil separation factor $(y_1 - y_4)/D$
λ_{suc}	Position factor of maximum suction $(y_3 - y_4)/(y_1 - y_4)$
f_{suc}	Maximum suction factor $-P_{suc}/P_{max}$
γ	Dunlap test parameter (Dunlap et al., 1990)
β	Dunlap test parameter (Dunlap et al., 1990)

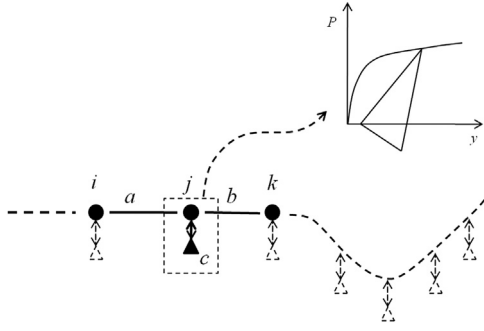


Fig. 3. Sketch of TDZ element attached to riser.

curve expressed as follows (Aubeny et al., 2006):

$$P = N_p D(S_0 + S_g y) \quad (7)$$

where N_p is a dimensionless bearing factor.

According to the linear hysteretic riser-seabed interaction model, a single point TDZ element is created and implanted in ABAQUS program. Fig. 3 shows the beam elements a and b connected to TDZ element c through the node j . According to the equilibrium equation, before the node j move downwards to point 1 in a loop shown in Fig. 2, element c has a positive stiffness and the riser is subjected to a resistance. After point 1, although node j keeps moving upwards, the stiffness of element c remains positive until node j reaches point 2. After point 2,

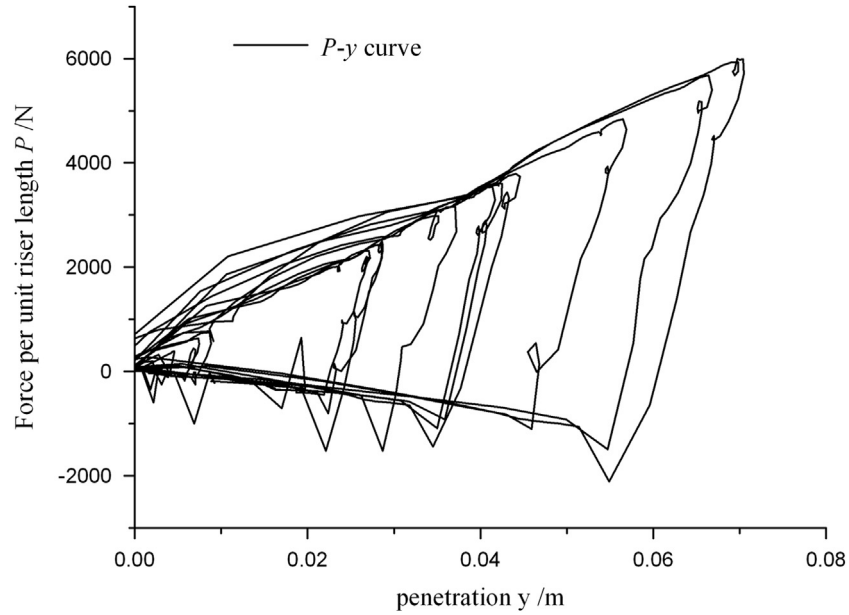


Fig. 4. Seabed force as a function of penetration at TDP.

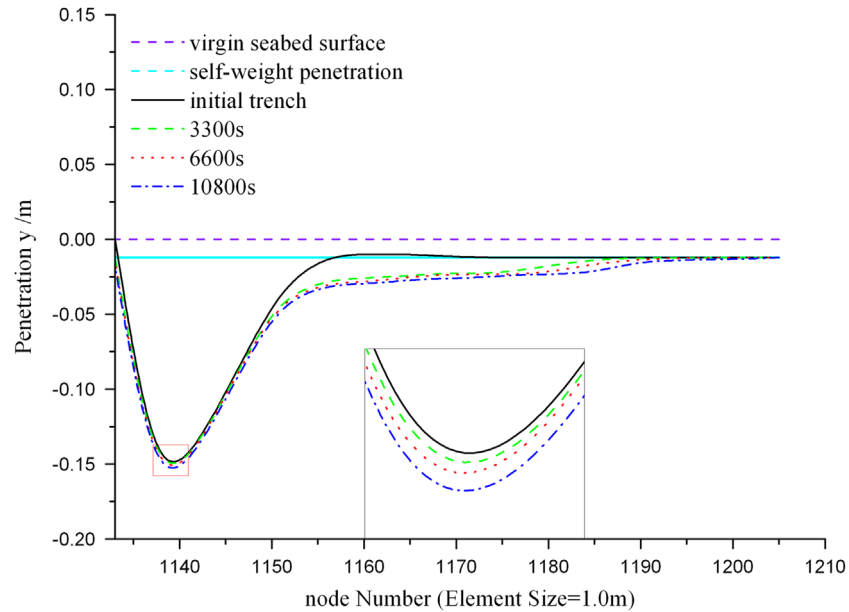


Fig. 5. Trench development.

a downward force is applied to the riser, which represents the suction of the clay.

4.2. Validation of the TDZ element

Assuming that S_0 and S_g are 2.5 kPa and 2.5 kPa/m respectively, f_{suc} is 0.2, and harmonic vertical response of SCR upper end with amplitude of 2m, a validation work is carried out to demonstrate the new element performance about the soil suction and seabed degradation. Fig. 4 shows that the mobilization and release of the suction are well captured, and the ratio of the maximum resistance to maximum suction is close to f_{suc} . Before the analysis, an initial trench is formed by assuming $y_{initial,max}$ of 0.145 m in the beam-spring model. After 3 h analysis, trenches with different depth are obtained as shown in Fig. 5. From the validation run, it is concluded that the riser-soil interaction phenomena can be well simulated by the proposed TDZ element.

Table 6
Information of seabed characteristic simulation.

Model number	Seabed characteristic	Sea state	Simulation time (s)
1	Linear stiffness K , considering riser-seabed separateness	All selected short term sea states	3600
2	Seabed mudline shear strength	sea state 6, $\alpha=0deg$	3600
3	Seabed shear strength gradient	sea state 6, $\alpha=0deg$	3600
4	Seabed suction effect	sea state 6, $\alpha=0deg$	3600
5	Trench depth effect	sea state 6, $\alpha=0deg$	3600

Table 7
Summary of seabed parameter values for 2nd~5th models.

Parameters	Model number			
	2	3	4	5
$y_{initial,max}$ (m)	0.2	0.2	0.2	0.3, 0.5, 0.7, 0.9
S_0 (kPa)	1.0, 2.0, 3.0, 3.5	1.5	1.25	1.5
S_g (kPa/m)	2.5	1.5, 2.5, 3.5, 4.5	2.5	2.5
μ_{sep}	1.0	1.0	1.0	1.0
λ_{suc}	0.7	0.7	0.7	0.7
f_{suc}	0.2	0.2	0.2, 0.3, 0.4, 0.6, 0.8	0.4
γ	2.0	2.0	2.0	2.0
β	0.002	0.002	0.002	0.002

5. Analysis results

The seabed characteristics, selected sea states and simulation time for this study are listed in Table 6, in which α represents the wave direction relative to the positive x -axial. The sea state 6 in the selected short term sea states is applied to study the influence of the 2nd–5th seabed characteristics on the fatigue damage. The relevant seabed parameters are presented in Table 7.

5.1. Linear stiffness considering riser-seabed separation

The TDZ element model can be simplified to a linear stiffness model considering riser-seabed separation. In this study, the different linear seabed stiffness is assumed to study its influence on the fatigue damage of a SCR at its TDP. They are 250 kN/m/m, 750 kN/m/m, 1250 kN/m/m and 1750 kN/m/m respectively. Fig. 6 gives the fatigue life as a function of the seabed stiffness. It indicates that higher seabed stiffness gives lower predicted

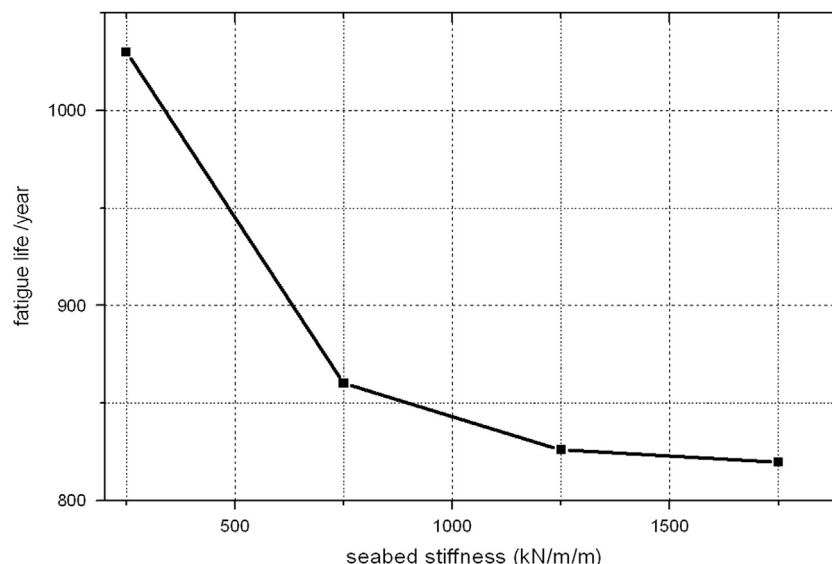


Fig. 6. Truncation linear stiffness effect on TDP's fatigue life.

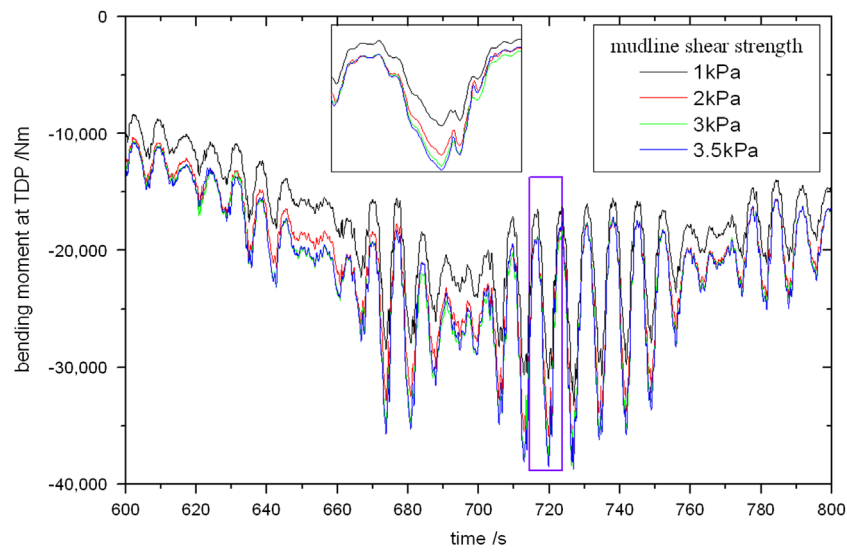


Fig. 7. Bending moment with different mudline shear strength S_0 and constant shear strength gradient $S_g = 2.5$ kPa/m.

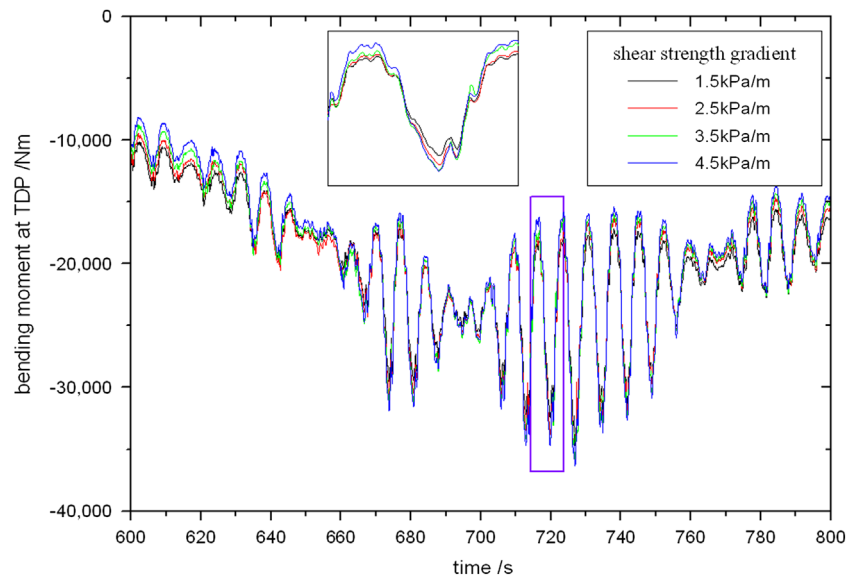


Fig. 8. Bending moment with different shear strength gradient S_g and constant mudline shear strength $S_0 = 1.5$ kPa.

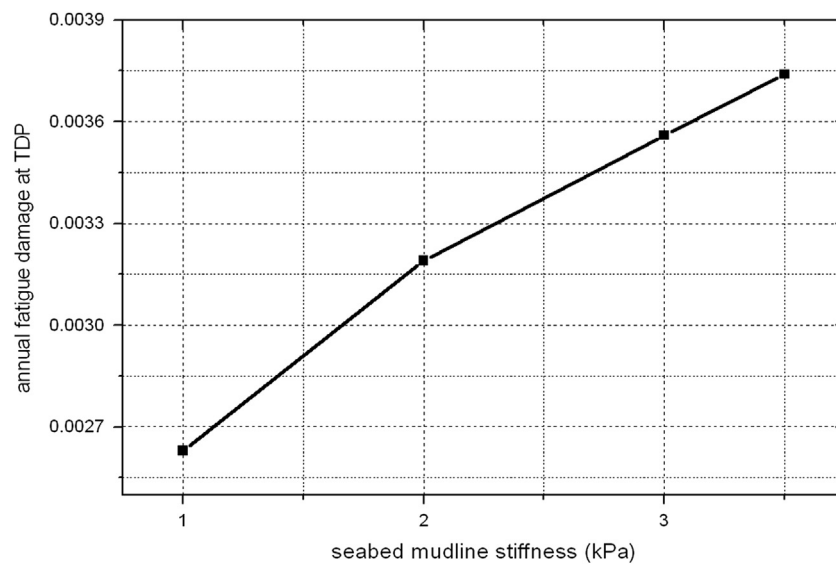


Fig. 9. Effect of mudline shear strength on fatigue damage at TDP.

fatigue life and the fatigue damage becomes less sensitive to the seabed stiffness as the stiffness increases.

5.2. Mudline shear strength and shear strength gradient

In the proposed linear hysteretic model, the maximum resistance of the seabed to the riser penetration during an entire cycle has a close relationship with the backbone curve which is mainly controlled by seabed mudline shear strength S_0 and shear strength gradient S_g . The fatigue sensitivity analyses are carried out by using the hysteretic model with a range of values of these two parameters. Fig. 7 shows that the mean value and amplitude of the bending moment range will increase as the seabed mudline shear strength increases. When the shear strength gradient increases, the bending moment range will increase associated with a nearly constant mean value as shown in Fig. 8. Figs. 9 and 10 indicate that the seabed mudline shear strength and shear strength gradient have a great influence on fatigue damage of a SCR at its TDP. As with the linear stiffness seabed model, higher mudline shear

strength and shear strength gradient, which corresponds to a stiffer seabed, will result in higher fatigue damage. The increment of the fatigue damage will decrease slightly as seabed mudline shear strength increases. In addition, the fatigue damage is almost linearly proportional to the shear strength gradient.

5.3. Soil suction

The force of clay soil applied to the riser is converted to suction rapidly when upward motion starts. In the linear hysteretic model, the maximum suction factor f_{suc} creates a bridge between the maximum suction and the maximum resistance. This study applies different suction factors to investigate the effect of suction on the riser response at the TDP. Figs 11 and 12 show that soil suction has a significant effect on the vertical displacement and bending moment of the SCR at its TDP. Larger suction will result in smaller amplitude of the vertical motion and larger bending moment range. Fig. 13 shows that the fatigue damage ratio to suction factor changes obviously at suction factor of 0.4. When the factor is

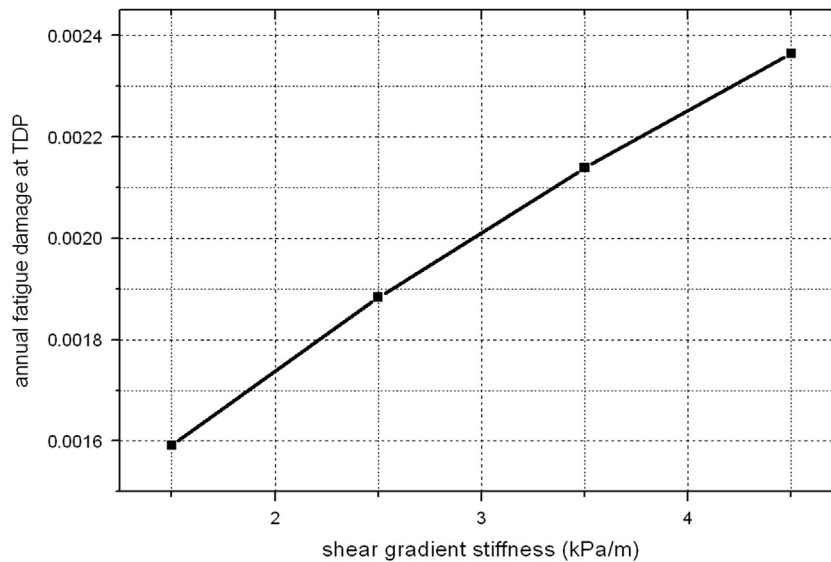


Fig. 10. Effect of shear strength gradient on fatigue damage at TDP.

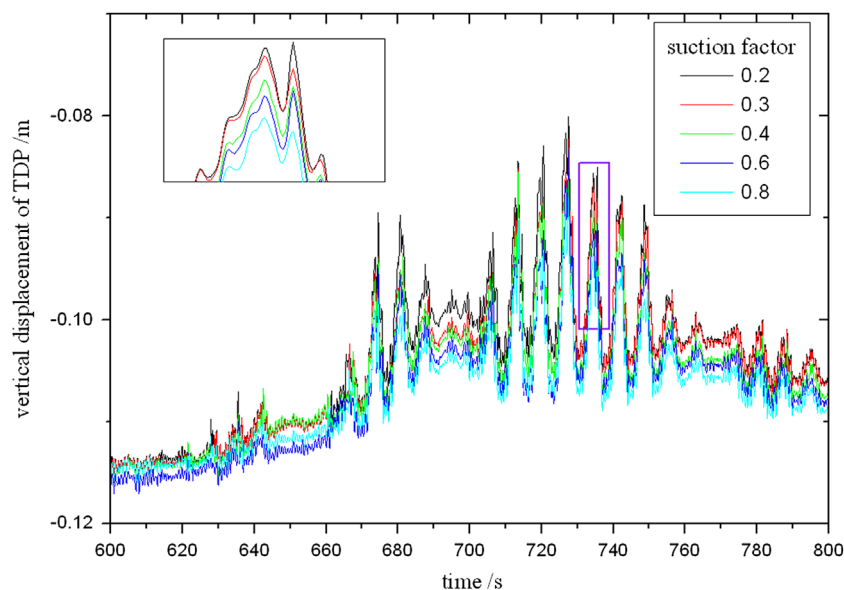


Fig. 11. Vertical displacement at the TDP with different suction factor.

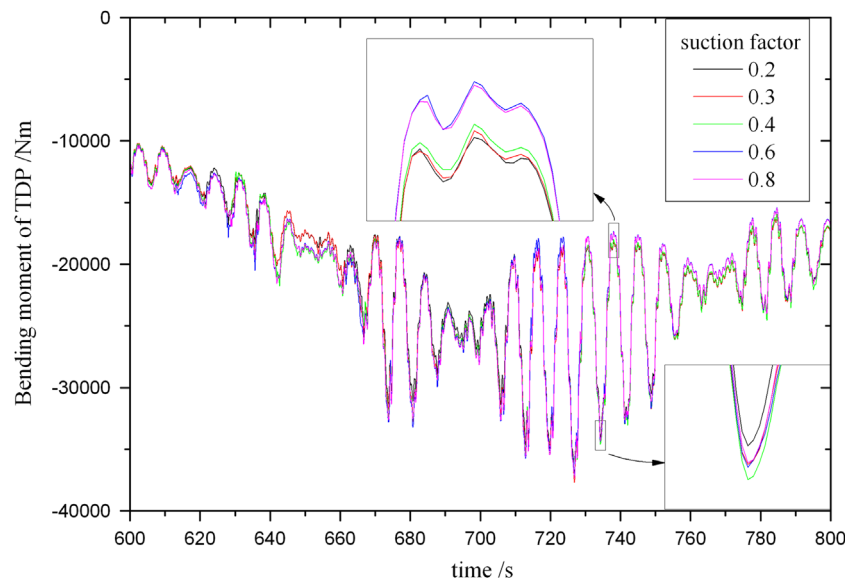


Fig. 12. Bending moment at the TDP about y-axis.

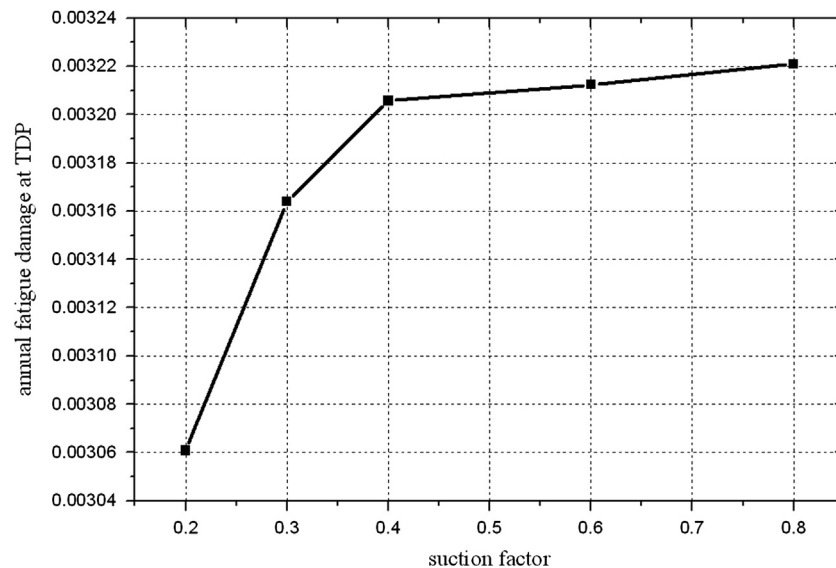


Fig. 13. Effect of suction factor on fatigue damage at the TDP.

greater than 0.4, fatigue damage will become less sensitive to the suction factor.

5.4. Trench depth

With the repeated interaction between riser and seabed, the trench becomes deeper and deeper and the bending moment of the riser at the TDP decreases gradually (Nakhaee and Zhang, 2010). The trench development is a very long process and the trench depth is expected to have a great impact on the fatigue damage of a SCR at its TDP. Four different $y_{initial,max}$ for beam-spring model are used to study the influence of the trench depth on fatigue damage at the TDP. In this study, a cycle with stress range equal to or greater than 15 MPa is defined as the high stress range cycle. Figs. 14 and 15 indicate that the number of high stress range cycles and fatigue damage will decrease as the trench depth

increases. Therefore, the trench development at the seabed is in favor of longer fatigue life of a SCR at its TDP.

6. Conclusion

Based on the proposed linear hysteretic riser-seabed interaction model, a TDZ element is created in ABAQUS/Standard using user-subroutine to investigate the effect of the seabed characteristics on fatigue damage of a SCR at its TDP. As a boundary condition in the global analysis, the upper end motion of the SCR is obtained through the coupled analysis of platform/mooring/riser system in Deep C. According to the fatigue analysis of the SCR with the particular geometry, some conclusions are summarized as follows:

1. The proposed TDZ element based on the linear hysteretic riser-soil interaction model in this study well captures some certain

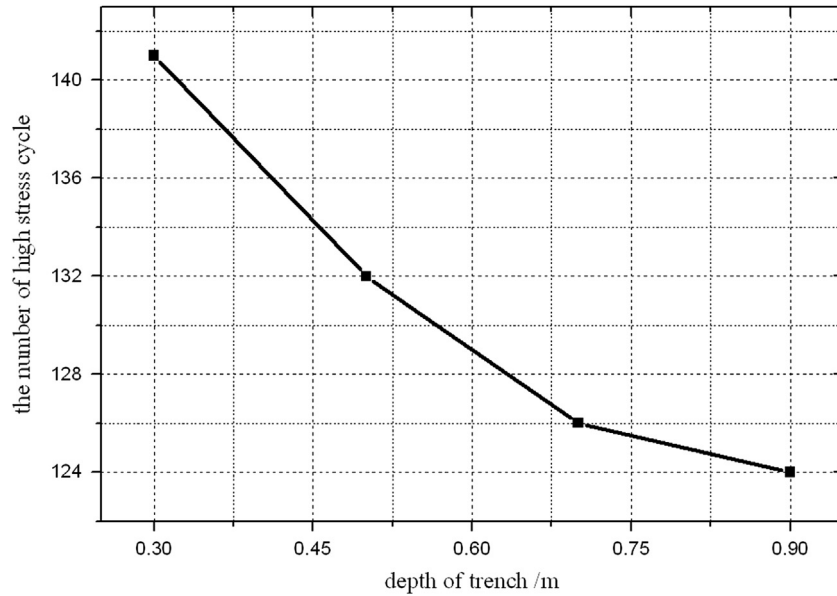


Fig. 14. The number of high stress range cycle.

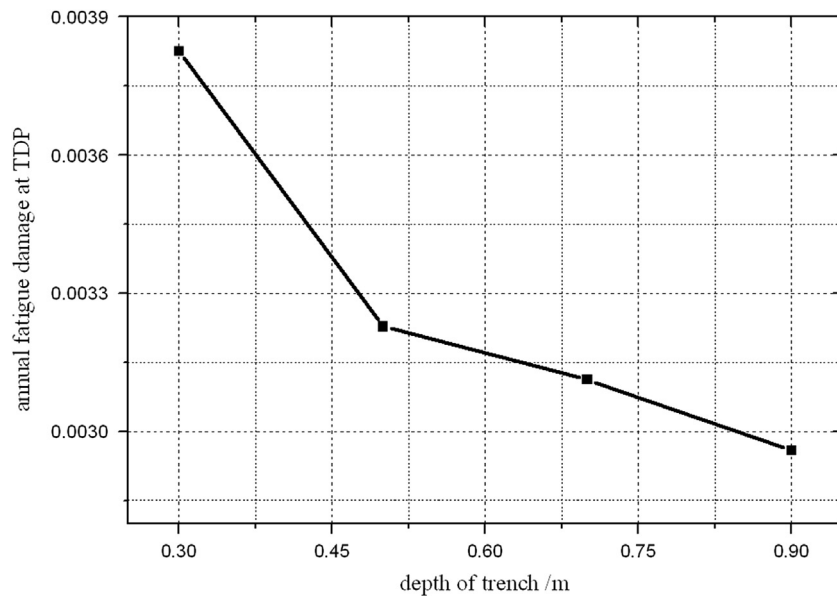


Fig. 15. Effect of trench depth on the fatigue damage at TDP.

phenomena, such as the mobilization and release of the clay suction, and the seabed degradation.

2. The seabed stiffness has a great influence on the predicted fatigue life of a SCR at its TDP. As the seabed linear stiffness increases, the predicted fatigue life will significantly decrease, and the rate of decrease will decline gradually. Therefore, the fatigue life of SCR at TDP is more sensitive to the seabed stiffness in a lower value range than to that in a higher value range.
3. Higher mudline shear strength gives higher mean value and range of bending moment at the TDP. Higher shear strength gradient results in higher bending moment range with a nearly constant mean value at the TDP. Higher mudline shear strength and higher shear strength gradient will lead to higher fatigue damage.
4. Soil suction will influence the riser response at the TDP. Larger suction results in lower amplitude of the vertical motion and

larger bending moment range. The suction factor of 0.4 is the critical point of the suction factor effect on fatigue damage of this SCR at the TDP. When the factor is greater than 0.4, fatigue sensitivity to the factor will decrease.

5. The deeper the trench, the less the number of high stress range cycle will be, so the trench development is in favor of the fatigue life of the SCR.
6. Using beam-spring model to form initial trench is a reasonable solution to simulate the trench with different depth since the trench development is very slow and the analysis time is limited in a fatigue analysis.

Compared with traditional models (Bridge and Laver, 2004), the proposed riser-soil interaction model in this study presents more realistic riser-soil interaction phenomena. Therefore, the predicted fatigue life is more reliable, which is very important for the SCR design.

Acknowledgment

This paper is based on the projects supported by the National Nature Science Foundation of China (Grant no. 51009089) and the Specialized Research Fund for the Doctoral Program of Higher Education of China (Grant no. 20100073120017). The authors also appreciate Dr. Xiaoyan Yan for her editorial help.

References

- 2H Offshore Engineering Ltd, 2002. STRIDE JIP—Effects of Riser/Seabed Interaction on SCRs. Report No. 1500-RPT-008.
- ABAQUS, 2005. ABAQUS Version 6.6.1 Documentation. ABAQUS, Inc. 1080 Main Street, Pawtucket, RI 02860, USA.
- Aubeny, C.P., Biscontin, G., Zhang, Jun, 2006. Seafloor Interaction with Steel Catenary Risers (Final Project Report). Texas: Texas A&M University.
- Aubeny, C.P., Biscontin, G., 2008. Interaction model for steel compliant riser on soft seabed. Offshore Technology Conference. Houston, Texas, USA: 19493-MS.
- Bridge, C., Laver, K., 2004. Steel catenary riser touchdown point vertical interaction models. Offshore Technology Conference. Houston, Texas, USA: 16628-MS.
- Bridge, C., Willis, N., 2002. Steel catenary risers—results and conclusions from large scale simulations of seabed interaction. In: Proceedings of the International Conference on Deep Offshore Technology, Penn Well.
- DNV, 2005a. Deep water coupled floater motion analysis (DeepC Theory). Norway.
- DNV, 2005b. Wave Analysis by Diffraction and Morison Theory (WADAM Theory). Norway.
- DNV, 2010a. Fatigue Design of Offshore Steel Structures, DNV-RP-C203.
- DNV, 2010b. Riser Fatigue. DNV-RP-F204.
- Dunlap, W.A., Bhojanala, R.P., Morris, D.V., 1990. Burial of vertically loaded offshore pipelines. Offshore Technology Conference. Houston, Texas.
- Fan, B.M., Ji, C.Y., Zhang, Q., 2008. Study on calculation method of deep-sea riser's fatigue life under wave and current combined operations. Ship and Ocean Engineering 37 (2), 91–94.
- Fu, J.J., Yang, H.Z., 2010. Fatigue characteristic analysis of deepwater steel catenary risers at the touchdown point. China Ocean Engineering 24 (2), 291–304.
- Larsen, C.M., Passano, E., 2006. Time and Frequency domain analysis of catenary risers subjected to vortex induced vibration. In: Proceedings of the 25th ASME OMAE Conference, Hamburg, Germany.
- Nakhaee, A., Zhang, Jun, 2010. Trenching effects on dynamic behavior of a steel catenary riser. Ocean Engineering 37, 277–288.
- Power, T.L., Maniar, D.R., Garrett, D.L., 2008. Spectral and cycle-counting fatigue damage estimation methods for steel catenary risers. Offshore Technology Conference. Houston, Texas, USA.
- Randolph, M., Quiggin P., 2009. Non-linear hysteretic seabed model for catenary pipeline contact. In: Proceedings of the ASME 28th International Conference on Ocean, Offshore and Arctic Engineering. Honolulu, Hawaii.
- Thethi, R., Moros, T., 2001. Soil interaction effects on simple catenary riser response. Deepwater Pipeline and Riser Technology Conference. Houston, Texas, USA.
- Willis, N.R.T., West, P.T.J., 2001. Interaction between deepwater catenary riser and a soft seabed: large scale sea trials. Offshore Technology Conference. Houston, Texas, USA.